Immunoreagents and competitive assays to fludioxonil

Antonio Abad-Fuentes,[a] Consuelo Agulló,[b] Francesc A. Esteve-Turrillas,[a] Antonio Abad-Somovilla,[b] Josep V. Mercader[a,*]

[a] *Department of Biotechnology, Institute of Agrochemistry and Food Technology, Consejo Superior de Investigaciones Científicas (IATA–CSIC), Agustí Escardino 7, 46980 Paterna, València, Spain*

[b] *Department of Organic Chemistry, Universitat de València, Doctor Moliner 50, 46100 Burjassot, València, Spain*

* Corresponding author: Tel.: +34-963900022; fax: +34-963636301.

E-mail address: jvmercader@iata.csic.es (J.V. Mercader).

Abstract

Fludioxonil is a new generation fungicide widely used for postharvest fruit protection. The aim of this study was to produce hitherto unreported immunoreagents for fludioxonil analysis by immunoassay. Derivatives of this agrochemical were synthesized with different linker tethering sites. Those functionalized haptens were activated, and the purified active esters were efficiently conjugated to different carrier proteins for immunogen and assay antigen preparation. Antibodies to fludioxonil were raised in rabbits and their selectivity and affinity were characterized, revealing the significance of the linker. Those antibodies were evaluated using homologous and heterologous conjugates by the direct and the indirect competitive ELISA formats. Finally, a pair of immunoreagents was identified showing an IC_{50} value for fludioxonil of 5.7 µg/L.

Keywords

Postharvest fungicide, hapten, active ester, immunoreagents, antibody, ELISA

INTRODUCTION

Research by the agrochemical industry has often been focused on natural occurring compounds in order to find novel active principles with adequate biocide activity and lower environmental and human health effects. With that aim, phenylpyrroles were investigated, and a synthetic derivative of pyrrolnitrin – an antibiotic produced by a number of *Pseudomonas* species – was launched as a last generation fungicide (*1*, *2*). This molecule was registered, in the mid '90s, under the name fludioxonil for postharvest treatment of stone fruit, pome fruit, pomegranate, kiwifruit, and citrus (*3*, *4*). Despite its reduced toxicity to humans, the proximity between application and consumption make exposure risks a concern. Chromatographic separation techniques coupled to mass spectrometry are commonly applied for fludioxonil residue analysis (*5*, *6*).

High-affinity antibody production for small chemicals, such as fludioxonil, demands accurate hapten design in order to mimic the electronic distribution and molecular conformation of the target analyte (*7*, *8*). Moreover, the main determinant chemical groups should be properly displayed to the immune system upon coupling to a carrier protein through a spacer arm with the adequate length (*9*). However, the optimum hapten derivatization site is still difficult to predict. The aim of the present study was to prepare different functionalized fludioxonil derivatives for producing selective and high-affinity antibodies. Generated immunoglobulins and conjugates of fludioxonil were evaluated by competitive enzyme-linked immunosorbent assay (cELISA) in order to select the best pair of immunoreagents for future assay development and sample analysis.

MATERIALS AND METHODS

Hapten Synthesis. Functionalized derivatives of fludioxonil (haptens FD*c* and FD*n*) were prepared as schematized in **Figures 1** and **2**. Experimental details and spectroscopic

characterization data of haptens and synthetic intermediates are provided in the Supporting Information.

Hapten activation and purification. Haptens were readily activated by formation of the corresponding *N*-hydroxysuccinimidyl ester (NHS-ester) using *N*,*N*'-disuccinimidyl carbonate (DSC) and triethylamine in dry acetonitrile as previously described (*10*). The activated hapten was straightforward purified by column chromatography, using $CHCl_3$ as eluent; affording the nearly pure NHS esters as determined by the ^1H NMR spectra (see the Supporting Information).

Conjugate Preparation and Antibody Production. Conjugation was carried out following standard procedures as described in the Supporting Information. Hapten-to-protein molar ratios (MR) were calculated from absorbance values of the conjugates and the protein at 280 nm. Animal manipulation was performed in compliance with the laws and guidelines of the Spanish Ministry of Agriculture, Fisheries, and Food, and approved by the Ethics Committee of the Universitat de València. Antibodies were generated in rabbits and purified from the antisera following regular protocols as described in the Supporting Information.

Competitive ELISAs. Assays were performed following common procedures for the antibody-coated direct and the conjugate-coated indirect cELISA formats, as previously published (*11*). Mean absorbance values (492 nm) were plotted versus the logarithm of analyte concentration, and assay sensitivity to fludioxonil was estimated as the analyte concentration reducing 50% (IC_{50}) the maximum absorbance (A_{max}).

RESULTS AND DISCUSSION

Hapten Synthesis. Two functionalized derivatives of fludioxonil were prepared, each of them holding the spacer arm at different sites of the pyrrole ring. Hapten FD*n* was easily obtained (overall yield 77%) from fludioxonil in two steps, which involved *N*-alkylation reaction of the pyrrole nitrogen atom with *tert*-butyl 6-bromohexanoate (**1**), to form the *N*-alkylated fluodioxonil derivative **2**, followed by acid hydrolysis of the *tert*-butyl ester group (**Figure 1**).

The synthesis of hapten FD*c* started with the transformation of the nitrile group of fludioxonil into a carboxylic acid group, which was carried out in two steps. First, the nitrile group was reduced to yield aldehyde **3**, whose subsequent oxidation provided carboxylic acid **4**. The carboxylated hydrocarbon chain that constituted the spacer arm was incorporated by coupling the carboxyl group of **4** with the amine group of **6**, previous derivatization of the carboxyl group to the corresponding *N*-succinimidyl ester, *e.g*. compound **5**. With amide **7** at hand, the synthesis of hapten FD*c* was readily finished by base-catalyzed hydrolysis of the methyl ester group. The complete synthetic route involved 5 steps and displayed an overall yield of 54% (**Figure 2**).

Hapten Activation and Conjugation. Hapten succinimidyl esters were readily prepared and purified in high yields (92% and 93% for FD*c*–NHS and FD*n*–NHS, respectively) using *N*,*N*'-disuccinimidyl carbonate. Activated purified haptens were coupled to bovine serum albumin (BSA), ovalbumin (OVA), and horseradish peroxidase (HRP). The amount of employed activated hapten was adjusted according to the desired final hapten density. Thus, high MRs for BSA conjugates (15 and 17 for FD*c* and FD*n*, respectively) and low MRs for OVA conjugates (2 for both haptens) were obtained as intended. On the other hand, calculated hapten densities of HRP conjugates were 6 and 4 for FD*c* and FD*n*, respectively. Unrealistic high MR values for HRP conjugates (this enzyme contains 3–4 available lysine residues) are

probably due to modified molar extinction coefficients of the protein and/or the hapten after conjugation. However, adequate enzymatic activity and hapten coupling was demonstrated by competitive assay.

Antibody Affinity and Selectivity. Competitive assays were performed with FD*c*-type antibodies (obtained with BSA–FD*c* as immunizing conjugate) and FD*n*-type antibodies (from BSA–FD*n* immunized animals), using homologous conjugates (same hapten as the immunizing conjugate) and following the direct and the indirect cELISA procedures. Antibody affinity was assessed by checkerboard competitive assays, running a standard curve of fludioxonil in each microplate column (from 10 pM to 10 μM plus a blank), and assaying diverse antibody and antigen concentrations simultaneously as described in the Supporting Information. The lowest IC_{50} values with homologous conjugates were obtained with antibodies from FD*n*-immunized rabbits in both cELISA formats (**Tables 1** and **2**). Thus, hapten FD*n* behaved better as immunogen than hapten FD*c*, so it was a better mimic of fludioxonil. Hapten FD*n* keeps unmodified all moieties of the target molecule, and only an N–H bond is substituted by an N–C bond. Comparatively, in hapten FD*c*, the cyano group modification probably alters more significantly the electronic properties of the pyrrole moiety (**Figures 1** and **2**). Moreover, the linker in hapten FD*n* is located further to the bulky aryl moiety than in hapten FD*c*, which probably favors that the aromatic portion of this hapten may adopt similar conformations to those adopted by the common framework of parent fludioxonil (see **Figure S1** of Supplementary Information).

Regarding selectivity, binding of the four antibodies to additional new generation fungicides which are commonly formulated together with fludioxonil was assessed, such as cyprodinil, pyrimethanil, mepanipyrim, azoxystrobin, boscalid, and fenhexamid. As expected,

no inhibition was observed by any of the studied compounds at a concentration of 10^4 nM with any of the described antibodies.

Competitive Immunoassays. Checkerboard assays were performed with both FD*c*- and FD*n*-type antibodies using also the heterologous conjugates. Concerning the direct cELISAs, antibody FD*c*#1 bound the heterologous tracer HRP–FD*n*, and a moderate IC_{50} value to fludioxonil was found in this case, improving the IC_{50} value that was obtained with the homologous combination. However, FD*n*-type antibodies recognized only the homologous tracer. Parallel results were observed with the indirect format (**Table 2**). For a particular antibody/antigen combination, the IC_{50} values stayed in the same order of magnitude in both cELISA formats. Overall, the most sensitive assay was achieved with antibody FD*n*#1 using the homologous combination. The inhibition curve of such assay is depicted in **Figure S2**, showing an IC_{50} value for fludioxonil of 22.9 nM (equivalent to 5.7 µg/L) and an A_{max} of 0.8 absorbance units.

ABBREVIATIONS USED

BSA: bovine serum albumin; cELISA: competitive enzyme-linked immunosorbent assay; DSC: *N*,*N*'-disuccinimidyl carbonate; HRP: horseradish peroxidase; MR: molar ratios; OVA: ovalbumin.

ACKNOWLEDGEMENTS

This work was supported by the Spanish *Ministerio de Ciencia e Innovación* (MICINN) (AGL2009-12940-C02-01/02/ALI) and cofinanced by FEDER funds. F.A.E.-T. and J.V.M. were hired by CSIC with postdoctoral contracts, the former under the JAE-doc program and the latter under the *Ramón y Cajal* program, both cofinanced by MICINN and by the European Social Fund (ESF). We thank Ana Izquierdo-Gil, Laura López-Sánchez, and Laura Vila-Dasí for excellent technical assistance.

Supporting Information Available: Synthesis details and characterization data of intermediates, haptens, and active esters. Equipment, immunoreagent production, ELISA procedures, fludioxonil most-stable conformations, and inhibition curve. This material is available free of charge via the Internet at http://pubs.acs.org.

LITERATURE CITED

(1) Schirra, M.; D'Aquino, S.; Cabras, P.; Angioni, A. Control of postharvest diseases of fruit by heat and fungicides: Efficacy, residue levels, and residue persistence. A review. *J. Agric. Food Chem.* **2011**, *59*, 8531–8542.

(2) Rosslenbroich, H. J.; Stuebler, D. *Botrytis cinerea* – history of chemical control and novel fungicides for its management. *Crop Prot.* **2000**, *19*, 557–561.

(3) Kanetis, L.; Förster, H.; Jones, C. A.; Borkovich, K. A.; Adaskaveg, J. E. Characterization of genetic and biochemical mechanisms of fludioxonil and pyrimethanil resistance in field isolates of *Penicillium digitatum*. *Phytopathology* **2008**, *98*, 205–214.

(4) Benigni, M.; Bompeix, G. Chemical and biological control of *Sclerotinia sclerotiorum* in witloof chicory culture. *Pest. Manag. Sci.* **2010**, *66*, 1332–1336.

(5) Cus, F.; Bach, B.; Barnavon, L.; Pongrac. V. Z. Analytical determination of Dolenjska region wines quality. *Food Control* **2013**, *33*, 274–280.

(6) Passarella, I.; Elia, I.; Guarino, B.; Bourlot, G.; Nègre, M. Evaluation of the field dissipation of fungicides and insecticides used on fruit bearing trees in northern Italy. *J. Environ. Sci. Heal B* **2009**, *44*, 137–143.

(7) Peterson, E. C.; Gunnell, M.; Che, Y.; Goforth, R. L.; Carroll, F. I.; Henry, R.; Liu, H.; Owens, S. M. Using hapten design to discover therapeutic monoclonal antibodies for treating methamphetamine abuse. *J. Pharmacol. Exp. Ther.* **2007**, *322*, 30–39.

(8) Mercader, J. V.; Agulló, C.; Abad-Somovilla, A.; Abad-Fuentes, A. Synthesis of site-heterologous haptens for high affinity anti-pyraclostrobin antibody generation. *Org. Biomol. Chem.* **2011**, *9*, 1443–1453.

(9) Mercader, J. V.; Suárez-Pantaleón, C.; Agulló, C.; Abad-Somovilla, A.; Abad-Fuentes, A. Hapten synthesis and monoclonal antibody-based immunoassay development for the detection of the fungicide kresoxim-methyl. *J. Agric. Food Chem.* **2008**, *56*, 1541–1552.

(10) Esteve-Turrillas, F. A.; Parra, J.; Abad-Fuentes, A.; Agulló, C.; Abad-Somovilla, A.; Mercader, J. V. Hapten synthesis, monoclonal antibody generation, and development of competitive immunoassays for the analysis of picoxystrobin in beer. *Anal. Chim. Acta* **2010**, *682*, 93–103.

(11) Mercader, J. V.; Esteve-Turrillas, F. A.; Agulló, C.; Abad-Somovilla, A.; Abad-Fuentes, A. Antibody generation and immunoassay development in diverse formats for pyrimethanil specific and sensitive analysis. *Analyst* **2012**, *137*, 5672–5679.

FIGURE CAPTIONS

Figure 1. Synthesis of hapten FD*n*.

Figure 2. Synthesis of hapten FD*c*. FD: fludioxonil.

Table 1. Assay sensitivity in the direct cELISA format.

	Tracer conjugate							
	HRP−FD*c*				HRP−FD*n*			
Ab	[Ab][a]	[C][b]	A_{max}	IC_{50}[c]	[Ab]	[C]	A_{max}	IC_{50}
FD*c*#1	30	3	1.0	1366.4	3	100	0.8	92.0
FD*c*#2	3	10	1.8	1542.6	3	100	---	---
FD*n*#1	3	100	---	---	10	3	0.8	22.9
FD*n*#2	3	100	---	---	30	10	1.2	129.5

[a] Antibody dilution ($\times 10^3$). [b] Conjugate concentration in ng/mL.
[c] Values in nM.

Table 2. Assay sensitivity in the indirect cELISA format.

	Coating conjugate							
	OVA−FD*c*				OVA−FD*n*			
Ab	[Ab][a]	[C][b]	A_{max}	IC_{50}[c]	[Ab]	[C]	A_{max}	IC_{50}
FD*c*#1	300	100	1.1	1405.7	10	1000	0.9	88.1
FD*c*#2	100	100	0.8	1329.4	10	1000	0.8	---
FD*n*#1	3	1000	---	---	30	100	1.5	75.1
FD*n*#2	3	1000	---	---	100	100	1.0	372.8

[a] Antibody dilution ($\times 10^3$). [b] Conjugate concentration in ng/mL.
[c] Values in nM.

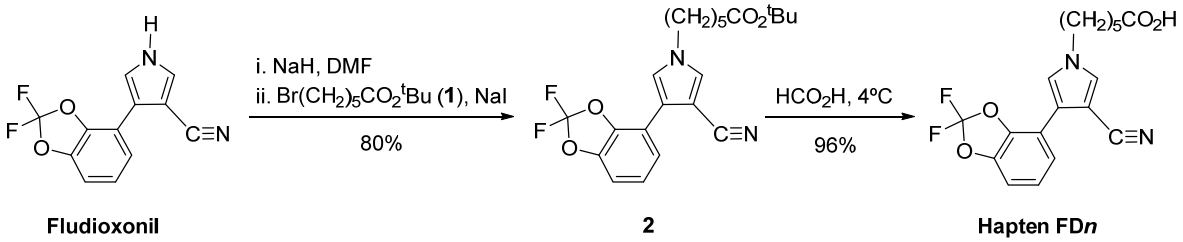

Fludioxonil **2** **Hapten FD*n***

Figure 1

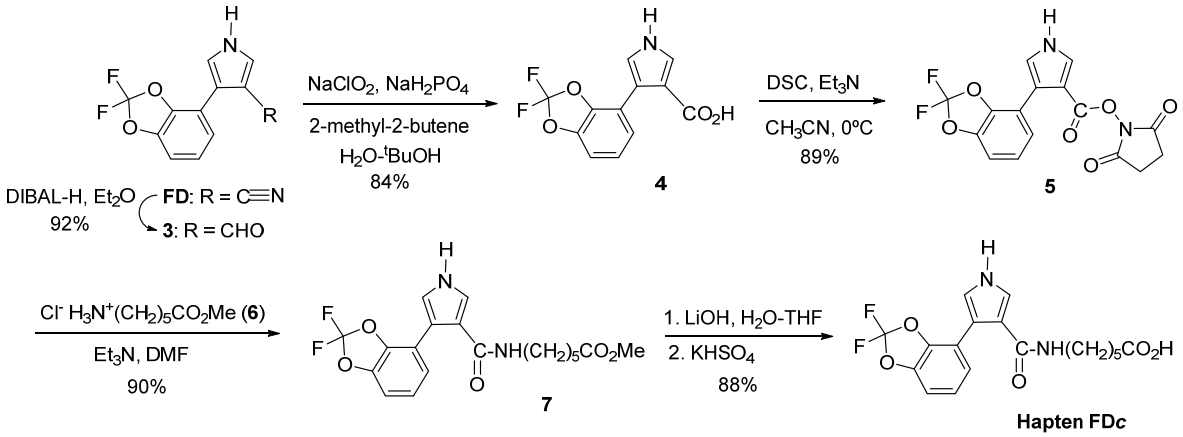
DIBAL-H, Et2O
92%
FD: R = C≡N
3: R = CHO
NaClO2, NaH2PO4
2-methyl-2-butene
H2O-tBuOH
84%
4
DSC, Et3N
CH3CN, 0ºC
89%
5
Cl- H3N+(CH2)5CO2Me (6)
Et3N, DMF
90%
7
1. LiOH, H2O-THF
2. KHSO4
88%
Hapten FDc

Figure 2

Supplementary Information

Immunoreagents and competitive assays to fludioxonil

General experimental details

The progress of reactions was monitored by thin layer chromatography (TLC) performed on F_{254} silica gel plates. The plates were visualized by immersion with ethanolic ceric ammonium molybdate or phosphomolybdic acid or aqueous sulphuric acid and heating. Column chromatography refers to flash chromatography and was performed on Merck silica gel 60, 230-400 mesh. All operations involving air-sensitive reagents were performed under an inert atmosphere of dry argon using syringe and cannula techniques, oven-dried glassware, and freshly distilled and dried solvents. Solvents and reagents were purified by standard methods.[1]

All melting points were determined using a Kofler hot-stage apparatus and are uncorrected. IR spectra were measured as KBr pellets or liquid films using a Nicolet Avatar 320 spectrometer. High-resolution mass spectra (HRMS) were run either by the electron impact (EI, 70 eV) obtained with a Micromass VG Autospec spectrometer, or the electrospray (ES) mode, which was obtained with a Q-TOF premier mass spectrometer with an electrospray source (Waters, Manchester, UK). ^{1}H NMR spectra were recorded on Bruker spectrometers, in the solvent indicated, at 300 MHz and ^{13}C NMR spectra at 75 MHz. ^{19}F NMR spectra were acquired at 282 MHz with high power proton decoupling. All proton and carbon spectra were referenced to residual solvent (^{1}H NMR: 7.26 ppm for $CDCl_3$, 3.58 ppm for THF-d_8, 3.31 ppm for MeOH-d_4, and 2.50 ppm for DMSO-d_6); ^{13}C NMR: 77.00 ppm for $CDCl_3$, 67.57 ppm for THF-d_8, 49.00 ppm for MeOH-d_4 and 39.52 ppm for DMSO-d_6). ^{19}F spectra were referenced to $CFCl_3$ as the internal reference which was set at δ 0.00 ppm. Carbon substitution degrees were established by DEPT pulse sequences. Complete assignment of ^{1}H and ^{13}C chemical shifts of selected compound in the synthetic sequence was made on the basis of a combination of COSY and HSQC experiments.

Synthesis of hapten FD*n*

The synthesis of hapten FD*n* is depicted Figure 1 of the article.

***tert*-Butyl 6-(3-cyano-4-(2,2-difluorobenzo[d][1,3]dioxol-4-yl)-1H-pyrrol-1-yl) hexanoate** (**2**). A solution of fluodioxonil (93.4 mg, 0.38 mmol) in DMF (0.4 mL) was added dropwise to a stirred suspension of prewashed (pentane) NaH (60% dispersion in mineral oil, 33 mg, 0.82 mmol) in anhydrous DMF (0.3 mL) under nitrogen. After stirring for 2 h at rt, a solution of sodium iodide (15.2 mg, 0.10 mmol) and *tert*-butyl 6-bromohexanoate (**1**, 142 mg, 0.56 mmol) in DMF (0.6 mL) was added and the mixture was stirred for an additional 3 h, then poured into water and extracted with ether. The combined organic layers were washed with a 2% aqueous solution of LiCl and brine and dried over anhydrous $MgSO_4$. The solvent

[1] Armarego, W. L. F.; Perrin, D. D. Purification of Laboratory Chemicals; 4th ed.; Oxford: Butterworth-Heinemann, 1996.

was removed under vacuum and the residue was chromatographed, using hexane-EtOAc mixtures (from 100:0 to 80:20), to give the ester **2** (126 mg, 80%) as an oil. IR (NaCl) ν_{max}/cm^{-1}: 3129, 2977, 2222, 1720, 1651, 1552, 1527, 1244, 1152, 763, 721. ^{1}H NMR (300 MHz, $CHCl_3$) δ (ppm): 7.70 (1H, dd, *J* = 8.1, 1.1 Hz), 7.25 (1H, d, *J* = 2.3 Hz), 7.14 (1H, d, *J* = 2.3 Hz), 7.12 (1H, dd, *J* = 8.1, 8.1 Hz), 6.95 (1H, dd, *J* = 8.1, 1.1 Hz), 3.95 (2H, t, *J* = 7.5 Hz), 2.22 (2H, t, *J* = 7.5 Hz), 1.84 (2H, quint, *J* = 7.4 Hz), 1.63 (2H, quint, *J* = 7.2 Hz), 1.42 (9H, s), 1.35 (2H, m). ^{13}C NMR (75 MHz, $CHCl_3$) δ (ppm): 172.6 (C), 143.7 (C), 139.7 (C), 131.3 (t, *J* = 255 Hz, C), 129.5 (CH), 124.0 (CH), 122.3 (CH), 121.2 (CH), 118.5 (C), 116.5 (C), 116.4 (C), 107.7 (CH), 91.0 (C), 80.2 (C), 50.4 (CH_2), 35.1 (CH_2), 30.7 (CH_2), 28.0 (CH_3), 25.8 (CH_2), 24.3 (CH_2). ^{19}F NMR (282 MHz, $CHCl_3$) δ (ppm): −49.96. HRMS (TOF MS ES+) *m/z*: calcd for $C_{22}H_{25}F_2N_2O_4$ $[M+H]^+$ 419.1782, found 419.1786.

6-(3-Cyano-4-(2,2-difluorobenzo[d][1,3]dioxol-4-yl)-1H-pyrrol-1-yl)hexanoic acid (**hapten FD*n***). *tert*-Butyl ester **2** (87 mg, 0.21 mmol) was dissolved in cooled (0 ºC) formic acid (2 mL) and the solution was stirred at 0–4 ºC for 3 h and then at rt for an additional 30 min. The reaction mixture was diluted with benzene and concentrated to dryness under vacuum (bath temperature not higher than 40 ºC). The residue was dissolved in benzene and the mixture concentrated again to dryness, to obtain hapten FD*n* (72 mg, 96%) as a white solid. Mp 100–102 ºC (crystallized from cool benzene–hexane). IR (NaCl) ν_{max}/cm^{-1}: 3500–2500, 3136, 2943, 2220, 1705, 1549, 1525, 1258, 1133, 762, 718. ^{1}H NMR (300 MHz, $CHCl_3$) δ: 11.2 (1H, br s), 7.71 (1H, dd, *J* = 8.1, 1.0 Hz), 7.24 (1H, d, *J* = 2.3 Hz), 7.15 (1H, d, *J* = 2.3 Hz), 7.13 (1H, dd, *J* = 8.1, 8.1 Hz), 6.96 (1H, dd, *J* = 8.1, 1.0 Hz), 3.97 (2H, t, *J* = 7.1 Hz), 2.39 (2H, t, *J* = 7.0 Hz), 1.87 (2H, quint, *J* = 7.3 Hz), 1.70 (2H, quint, *J* = 7.2 Hz), 1.39 (2H, m). ^{13}C NMR (75 MHz, $CHCl_3$) δ (ppm): 179.4 (C), 143.8 (C), 139.7 (C), 131.3 (t, *J* = 255 Hz, C), 129.5 (CH), 124.0 (CH), 122.3 (CH), 121.2 (CH), 118.6 (C), 116.5 (C), 116.4 (C), 107.7 (CH), 91.0 (C), 50.4 (CH_2), 33.6 (CH_2), 30.6 (CH_2), 25.8 (CH_2), 23.9 (CH_2). ^{19}F NMR (282 MHz, $CHCl_3$) δ (ppm): −49.95. HRMS (TOF-MS–ES+) *m/z*: calcd for $C_{18}H_{17}F_2N_2O_4$ $[M+H]^+$ 363.1156, found 363.1151.

Synthesis of hapten FD*c*

The synthesis of hapten FD*c* is depicted Figure 2 of the article.

4-(2,2-Difluorobenzo[d][1,3]dioxol-4-yl)-1H-pyrrole-3-carbaldehyde (**3**). A solution of DIBAL-H in toluene (1M, 2.3 mL, 2.3 mmol) was dropwise added to a solution of fludioxonil (400 mg, 1.61 mmol) in anhydrous Et_2O (20 mL) at −60 ºC under nitrogen. The reaction mixture was stirred while it was allowed to warm to −30 ºC during the course of 1 h and kept at this temperature for 30 min, then the cooling bath was retired and the reaction mixture stirred for 1 h. After this time, the reaction mixture was transferred via cannula to a slurry of silica gel (1.8 g) in water (0.7 mL), cooled at 0 ºC, and the mixture stirred at this temperature

for 1 h and then at rt for an additional 1 h. Solid K_2CO_3 (2.68 g) and $MgSO_4$ (2.68 g) were added and the stirring was continued for another 1 h, then filtered under vacuum using a Büchner funnel and the filtrate and washings were concentrate to dryness to give the aldehyde **3** (371 mg, 92%) as a solid, which was used to the next step without further purification. Mp 143.7–146.1 ºC (from hexane-EtOAc). IR (KBr) ν_{max}/cm^{-1}: 3281, 3924, 1659, 1453, 1317, 1233, 1133, 1099, 1050, 762, 716. ^{1}H NMR (300 MHz, $CDCl_3$) δ (ppm): 9.93 (1H, s), 8.88 (1H, br s), 7.56 (1H, dd, *J* = 3.2, 2.2 Hz), 7.44 (1H, dd, *J* = 8.1, 1.2 Hz), 7.17 (1H, dd, *J* = 2.2, 2.2 Hz), 7.12 (1H, dd, *J* = 8.0, 8.0 Hz), 6.99 (1H, dd, *J* = 8.0, 1.2 Hz). ^{13}C NMR (75 MHz, $CDCl_3$) δ (ppm): 185.6 (CH), 143.7 (C), 140.9 (C), 131.4 (t, *J* = 254 Hz, C), 128.5 (CH), 125.0 (CH), 123.8 (C), 123.4 (CH), 121.0 (CH), 117.4 (C), 117.2 (C), 107.9 (CH). ^{19}F NMR (282 MHz, $CHCl_3$) δ (ppm): −50.17. HRMS (TOF MS ES+) *m/z*: calcd for $C_{12}H_8F_2NO_3$ $[M+H]^+$ 252.0472, found 252.0478.

4-(2,2-Difluorobenzo[d][1,3]dioxol-4-yl)-1H-pyrrole-3-carboxylic acid (**4**). A solution of $NaClO_2$ (800 mg, 8.84 mmol), and $NaH_2PO_4{\cdot}H_2O$ (1.129 g, 1.18 mmol) in water (3.2 mL) and 2-methyl-2-butene (836 mg, 1.26 mL 11.92 mmol) were consecutively added to a solution of aldehyde **3** (318.6 mg, 1.27 mmol) in *tert*-BuOH (2.5 mL) cooled to 0 ºC. The reaction flask was tightly closed and the mixture was allowed to warm to rt and stirred overnight. The reaction mixture was poured into water and extracted with Et_2O. The ethereal layer was extracted with a 1 M solution of NaOH and the ethereal layer was washed with brine, dried over anhydrous $MgSO_4$ and concentrated to afford unreacted starting aldehyde **3** (29.9 mg, 9.4%). The aqueous layer was acidified to pH 4–5 with citric acid and extracted with Et_2O. The combined organic layer were washed with brine, dried over anhydrous $MgSO_4$ and concentrated to dryness under vacuum to afford the acid **4** [268.1 mg, 84% (93% based on recovered starting material)] as a solid that was pure enough to be used in the next step without further purification. Mp 188–189.0 ºC (from hexane-EtOAc). IR (KBr) ν_{max}/cm^{-1}: 3500–2500, 3126, 2885, 1668, 1535, 1454, 1241, 1156, 780, 578. ^{1}H NMR (300 MHz, DMSO-d_6) δ (ppm): 11.84 (1H, br s), 11.65 (1H, br s), 7.47 (1H, dd, *J* = 2.7, 2.4), 7.25–7.14 (3H, m), 7.02 (1H, t, *J* = 2.4, 2.4). ^{13}C NMR (75 MHz, DMSO-d_6) δ (ppm): 165.1 (C), 142.4 (C), 140.6 (C), 130.9 (t, *J* = 251 Hz, C), 125.5 (CH), 125.4 (CH), 123.3 (C), 120.1 (CH), 119.3 (C), 116.4 (C), 113.8 (C), 107.5 (CH). ^{19}F NMR (282 MHz, DMSO-d_6) δ (ppm): −49.26. HRMS (TOF MS ES-) *m/z*: calcd for $C_{12}H_7F_2NO_4$ $[M-H]^+$ 266.0265, found 266.0269.

Methyl 6-(4-(2,2-difluorobenzo[d][1,3]dioxol-4-yl)-1H-pyrrole-3-carboxamido) hexanoate (**7**). Anhydrous Et_3N (409 μL, 297 mg, 2.93 mmol) was added to a solution of acid **4** (206.5 mg, 0.773 mmol) and *N,N*′-disuccinimidyl carbonate (DSC, 257 mg, 1.00 mmol) in anhydrous CH_3CN (7 mL) at 0 ºC under nitrogen and the mixture was stirred at this temperature for 2 h. The solvent and the excess Et_3N were eliminated at reduced pressure, and the residue was purified by column chromatography, eluting first with CH_2Cl_2 and then

with $CHCl_3$, to give the succinimidyl ester intermediate **5** (250.6 mg, 89%). ^{1}H NMR (300 MHz, $CHCl_3$) δ (ppm): 9.59 (1H, br s), 7.65 (1H, dd, *J* = 3.3, 2.1), 7.21 (1H, dd, *J* = 8.1, 1.5 Hz), 7.02 (1H, dd, *J* = 8.1, 8.1 Hz), 7.00 (1H, dd, *J* = 3.3, 1.5 Hz), 6.94 (1H, dd, *J* = 8.1, 1.5 Hz), 2.86 (4H, s).

A solution of methyl 6-amino-hexanoate hydrochloride (**6**, 152.6 mg, 0.84 mmol) and Et_3N (129 μL, 93.5 mg, 0.924 mmol) in anhydrous DMF (4 mL) was added to a solution of the above obtained succinimidyl ester **5** (102 mg, 0.280 mol) in DMF (0.5 mL). The mixture was stirred at rt for 4 h, diluted with water and extracted with Et_2O. The combined organic extracts were washed with a 2% aqueous solution of LiCl and brine and dried over anhydrous $MgSO_4$. Chromatographic purification of the residue left after evaporation of the solvent, using $CHCl_3$ as eluent, afforded the amide **7** (99.5 mg, 90%) as an oil. IR (KBr) ν_{max}/cm^{-1}: 3335, 3131, 2947, 1736, 1653, 1603, 1561, 1458, 1239, 1144, 1110, 771. ^{1}H NMR (300 MHz, $CDCl_3$) δ (ppm): 9.92 (1H, br s), 7.32 (1H, dd, *J* = 2.3, 2.3 Hz), 7.15 (1H, dd, *J* = 7.9, 1.3 Hz), 7.06 (1H, dd, *J* = 7.9, 7.9 Hz), 6.96 (1H, dd, *J* = 7.9, 1.3 Hz), 6.90 (1H, dd, *J* = 2.3, 2.3 Hz), 5.66 (1H, br t, *J* = 5.5 Hz), 3.64 (3H, s), 3.30 (2H, q, *J* = 6.9 Hz), 2.26 (2H, t, *J* = 7.4 Hz), 1.59 (2H, t, quint, *J* = 7.4 Hz), 1.45 (2H, m), 1.24 (2H, m). ^{13}C NMR (75 MHz, $CDCl_3$) δ (ppm): 174.1 (C), 165.7 (C), 143.7(C), 141.0 (C), 131.3 (t, *J* = 252 Hz, C), 124.7 (CH), 123.5(CH), 122.4 (C), 119.7 (CH), 118.3 (C), 118.2 (C), 114.6 (C), 107.7 (CH), 51.5 (OCH_3), 39.3 (CH_2), 33.8 (CH_2), 29.1 (CH_2), 26.3 (CH_2), 24.5 (CH_2). ^{19}F NMR (282 MHz, $CHCl_3$) δ (ppm): −50.07. HRMS (TOF MS ES-) *m/z*: calcd for $C_{19}H_{20}F_2N_2O_5$ $[M-H]^+$ 393.1262, found 393.1258.

6-(4-(2,2-Difluorobenzo[d][1,3]dioxol-4-yl)-1H-pyrrole-3-carboxamido)hexanoic acid (**hapten FD*c***). A solution of the methyl ester **7** (112.5 mg, 0.285 mmol) in a mixture of THF (2.3 mL) and H_2O (0.95 mL) was treated with $LiOH{\cdot}H_2O$ (120.4 mg, 2.869 mmol) and stirred at rt for 2.5 h. The reaction mixture was diluted with H_2O (20 mL) and extracted with ethyl ether. The organic layer was discarded and the aqueous layer was evaporated under vacuum to eliminate the remains of organic solvent, then cooled in an ice bath and acidified with a saturated aqueous solution of $KHSO_4$ to approximately pH 3. The precipitate formed was filtered off, washed with water and dried to afford the hapten FD*c* (96 mg, 88%) as a semi-solid. IR (KBr) ν_{max}/cm^{-1}: 3500–2500, 2936, 1712, 1654, 1605, 1544, 1453, 1235, 1149, 723. ^{1}H NMR (300 MHz, THF-d_8) δ (ppm): 10.7 (1H, br s), 7.42 (1H, dd, *J* = 8.1, 1.5 Hz), 7.17 (1H, dd, *J* = 2.7, 2.4 Hz), 7.04 (1H, dd, *J* = 7.8, 7.8 Hz), 6.98–6.94 (2H, a dd overlapped with other dd of *J* = 8.1, 1.2 Hz), 6.83 (1H, br t, *J* = 5.7 Hz), 3.25 (2H, q, *J* = 6.5 Hz), 2.21 (2H, t, *J* = 7.5 Hz), 1.53 (4H, m), 1.35 (2H, m). ^{13}C NMR (75 MHz, THF-d_8) δ (ppm): 174.7 (C), 165.9 (C), 144.4 (C), 141.6 (C), 132.5 (t, *J* = 253 Hz, C), 126.3(CH), 124.0 (CH), 122.1 (CH), 120.8 (C), 120.6 (CH), 120.4 (C), 116.2 (C), 107.3 (CH), 40.0 (CH_2), 34.3 (CH_2), 30.6 (CH_2), 27.7

(CH_2), 25.8 (CH_2). ^{19}F NMR (282 MHz, THF-d_8) δ (ppm): −45.78. HRMS (TOF MS ES+) *m/z*: calcd for $C_{18}H_{19}F_2N_2O_5$ $[M+H]^+$ 381.1262, found 381.1260.

^{1}H NMR spectra of NHS-esters of haptens FD*c* and FD*n*

FD*c*–NHS ester (1 h at 0 °C; 92% yield): ^{1}H-NMR (300 MHz, $CDCl_3$) δ (ppm) 9.42 (1H, br s), 7.30 (1H, dd, *J* = 2.8, 2.3 Hz), 7.17 (1H, dd, *J* = 7.9, 1.3 Hz), 7.09 (1H, dd, *J* = 7.9, 7.9 Hz), 6.97 (1H, dd, *J* = 7.9, 1.3 Hz), 6.94 (1H, dd, *J* = 2.3, 2.3 Hz), 5.74 (1H, t, *J* = 5.7 Hz), 3.31 (2H, q, *J* = 6.5 Hz), 2.81 (4H, br s), 2.56 (2H, t, *J* = 7.3 Hz), 1.72 (2H, t, quint, *J* = 7.1 Hz), 1.49 (2H, quint, *J* = 7.1 Hz), 1.35 (2H, m).

FD*n*–NHS ester (4 h at room temperature; 93% yield): ^{1}H-NMR (300 MHz, $CDCl_3$) δ (ppm) 7.71 (1H, dd, *J* = 8.2, 1.1 Hz), 7.26 (1H, d, *J* = 2.0 Hz), 7.16 (1H, d, *J* = 2.0 Hz), 7.12 (1H, dd, *J* = 8.1, 8.1 Hz), 6.96 (1H, dd, *J* = 8.1, 1.1 Hz), 3.97 (2H, t, *J* = 7.1 Hz), 2.84 (4H, br s), 2.63 (2H, t, *J* = 7.1 Hz), 1.85 (4H, m), 1.47 (2H, m).

Chemicals and instrumentation

Pestanal grade fludioxonil (4-[2,2-difluoro-1,3-benzodioxol-4-yl]-1*H*-pyrrole-3-carbonitrile, CAS registry number 131341-86-1, Mw 249.19) was purchased from Fluka/Riedel-de-Haën (Seelze, Germany). Other chemicals were obtained from standard sources. Bovine serum albumin (BSA) fraction V was from Roche Applied Science (Mannheim, Germany). Ovalbumin (OVA) and horseradish peroxidase (HRP) were purchased from Sigma/Aldrich (Madrid, Spain).

Sephadex G-25 HiTrap Desalting columns from GE Healthcare (Uppsala, Sweden) were utilized for protein–hapten conjugate purification. Costar flat-bottom high-binding 96-well polystyrene ELISA plates were from Corning (Corning, NY, USA). UV–visible spectra and ELISA absorbances were read with a PowerWave HT from BioTek Instruments (Winooski, VT, USA). Microwells were washed with an ELx405 microplate washer also from BioTek Instruments.

Hapten activation

The hapten (1 equiv) and DSC (1.3 equiv) were dissolved in anhydrous acetonitrile (1 mL per 0.1 mmol of hapten) under nitrogen in an ice-water bath. Triethylamine (3.5 equiv) was then added, and the resulting mixture was stirred at 0 °C or at room temperature for haptens FD*c* and FD*n*, respectively, until complete consumption of the starting material (as observed by thin layer chromatography using $CHCl_3$:MeOH 9:1 as eluent). The reaction mixture was diluted with $CHCl_3$, washed with a 10% aqueous solution of $NaHCO_3$ and brine, and dried over anhydrous Na_2SO_4. After evaporation of the solvent, the activated hapten was purified by column chromatography, using $CHCl_3$ as eluent.

Conjugate preparation

Conjugation was carried out in carbonate buffer, pH 9.6, during 2 h under moderate stirring at room temperature. Immunizing conjugates were prepared by reaction of 10 μmol of purified activated hapten in DMF (100 μL) with 30 mg of BSA in carbonate buffer (2 mL). For coating conjugates, 2 μmol of activated hapten in DMF (100 μL) was conjugated to 30 mg of OVA in the described buffer (2 mL), whereas for enzyme assay conjugates, 0.5 μmol of active ester solution in DMF (50 μL) was reacted with 2.2 mg of HRP in carbonate buffer (1 mL). Conjugates were purified by gel filtration chromatography using 100 mM phosphate buffer, pH 7.4 as eluent. BSA and OVA conjugates were stored frozen at −20 °C, and HRP conjugates were kept at 4 °C.

Antibody production

With each immunogen, two antisera were generated from two 2-kg female New Zealand white rabbits, which had been immunized, with 21-day intervals, by subcutaneous injection of 0.3 mg of BSA–hapten conjugate in 1 mL of a 1:1 emulsion between 100 mM phosphate, pH 7.4, and Freund's adjuvant (complete for the first dose and incomplete for subsequent boosts). Ten days after the fourth injection, rabbits were exsanguinated. Blood samples were allowed to coagulate overnight at 4 °C, and sera were separated by centrifugation. Finally, antibodies were precipitated with 1 volume of saturated ammonium sulfate solution. Salting out was performed twice, and precipitates were stored at 4 °C.

Checkerboard competitive assays

For the direct format, three different antibody dilutions (1/3000, 1/10000, and 1/30000) and four enzyme tracer concentrations (3, 10, 30, and 100 ng/mL) were assayed in the same plate. For indirect competitive assays, plates were coated with 100 or 1000 ng/mL OVA conjugate, and diverse antibody dilutions were assayed from 1/3000 to 1/300000 in one plate. Consequently, 12 inhibition curves were retrieved from every plate; each curve corresponding to a particular antibody and assay conjugate concentration. Absorbance was read immediately after assays at 492 nm with a reference wavelength at 650 nm. Experimental values were fitted to a four-parameter logistic equation using the SigmaPlot software package from SPSS Inc. (Chicago, IL, USA).

Figure S1

Graph of potential energy of fludioxonil as a function of the dihedral angle between the benzene and pyrrole rings and its most stable conformations (arrows denote the attachment site of the spacer arm in the immunizing haptens).

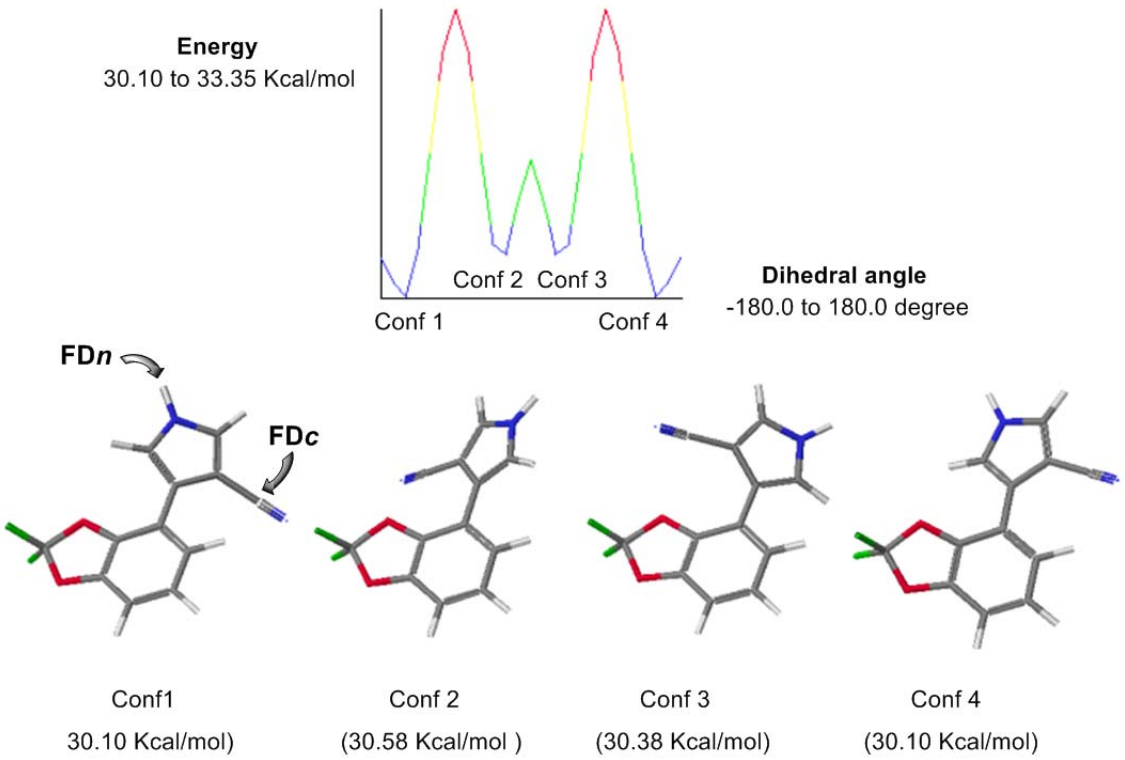

Figure S2

Inhibition curve obtained with antibody FD*n*#1 and tracer HRP–FD*n* in the direct cELISA format. Values are the mean of three independent replicates.

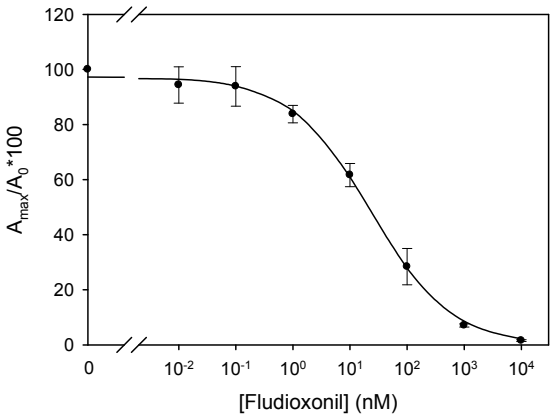

^{1}H NMR spectra of NHS-esters of haptens FD*c* and FD*n*

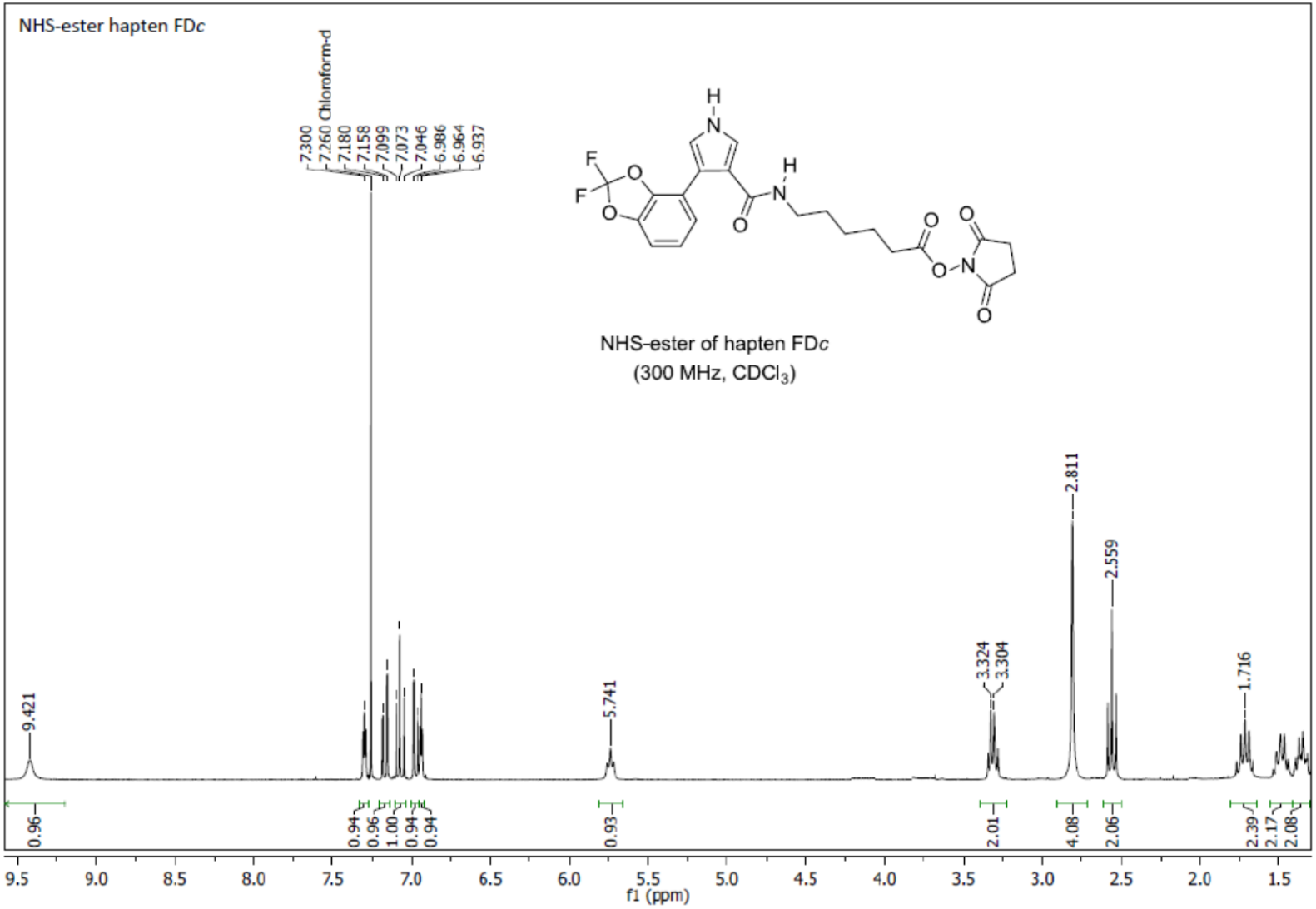
NHS-ester hapten FDc
7.300
7.260 Chloroform-d
7.180
7.158
7.099
7.073
7.046
6.986
6.964
6.937
NHS-ester of hapten FDc
(300 MHz, CDCl3)
9.421
5.741
3.324
3.304
2.811
2.559
1.716
0.96
0.94
0.96
1.00
0.94
0.94
0.93
2.01
4.08
2.06
2.39
2.17
2.08
9.5
9.0
8.5
8.0
7.5
7.0
6.5
6.0
5.5
5.0
4.5
4.0
3.5
3.0
2.5
2.0
1.5
f1 (ppm)

2

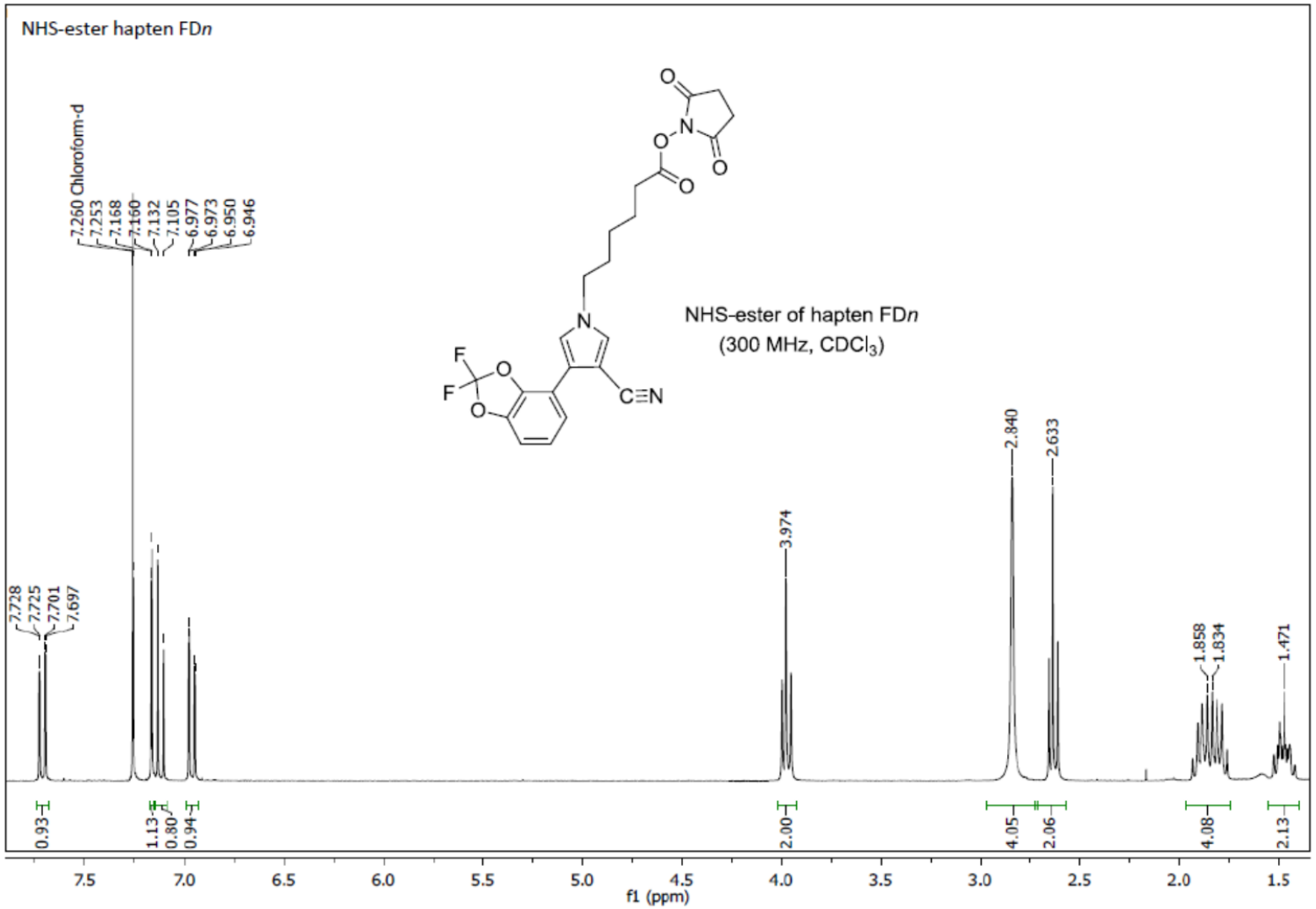
NHS-ester hapten FDn
7.260 Chloroform-d
7.253
7.168
7.160
7.132
7.105
6.977
6.973
6.950
6.946
7.728
7.725
7.701
7.697
3.974
2.840
2.633
1.858
1.834
1.471
NHS-ester of hapten FDn
(300 MHz, CDCl3)
0.93
1.13
0.80
0.94
2.00
4.05
2.06
4.08
2.13
f1 (ppm)

3

4